nanomaterials

MDPI

Article

Spectroscopic Study of the Salicyladazine Derivative–UO_2^{2+} Complex and Its Immobilization to Mesoporous Silica

Sujin Park [1], Jaehyeon Park [1], Ji Ha Lee [2,*], Myong Yong Choi [1,*] and Jong Hwa Jung [1,*]

[1] Department of Chemistry and Research Institute of Natural Sciences, Gyeongsang National University, Jinju 52828, Korea; 0165255562@naver.com (S.P.); parkjae@gnu.ac.kr (J.P.)
[2] Department of Chemistry and Biochemistry, The University of Kitakyushu, Hibikino, Kitakyushu 808-0135, Japan
* Correspondence: l-ji@kitakyu-u.ac.jp (J.H.L.); mychoi@gnu.ac.kr (M.Y.C.); jonghwa@gnu.ac.kr (J.H.J.); Tel.: +82-55-772-1488 (J.H.J.)

Received: 2 April 2019; Accepted: 26 April 2019; Published: 2 May 2019

Abstract: Uranyl ion, the most soluble toxic uranium species, is recognized as an important index for monitoring nuclear wastewater quality. The United States Environmental Protection Agency (US EPA) and the World Health Organization (WHO) prescribed 30 ppb as the allowable concentration of uranyl ion in drinking water. This paper reports on a nanohybrid material that can detect uranyl ions spectroscopically and act as a uranyl ion absorbent in an aqueous system. Compound **1**, possessing a salicyladazine core and four acetic acid groups, was synthesized and the spectroscopic properties of its UO_2^{2+} complex were studied. Compound **1** had a strong blue emission when irradiated with UV light in the absence of UO_2^{2+} that was quenched in the presence of UO_2^{2+}. According to the Job's plot, Compound **1** formed a 1:2 complex with UO_2^{2+}. When immobilized onto mesoporous silica, a small dose (0.3 wt %) of this hybrid material could remove 96% of UO_2^{2+} from 1 mL of a 100-ppb UO_2^{2+} aqueous solution.

Keywords: UO_2^{2+}; salicyladazine; fluorescence; mesoporous silica

1. Introduction

The development of nuclear technology leads to new environmental concerns, such as radiation exposure and accidents resulting therefrom. Of special concern is the uranyl cation (UO_2^{2+}), a highly toxic neurotoxin that is very mutable in biological systems and can cause radioactive poisoning if proper containment rules are violated [1–4]. Therefore, the development of technologies that can measure the exact amount of UO_2^{2+} exposed to the environment is an important safety priority.

Several studies on UO_2^{2+} sensors have been reported to date [5–10]. L. S. Natrajan et al. reported a method for detecting UO_2^{2+} via a unique fluorescence energy transfer process to a water-soluble europium (III) lanthanide complex triggered by UO_2^{2+} [11]. Yi Lu et al. developed colorimetric uranium sensors based on a UO_2^{2+}-specific DNAzyme and gold nanoparticles using both labeled and label-free methods [12]. Julius Rebek Jr. et al. investigated a tripodal receptor capable of extracting uranyl ion from aqueous solutions. In their system, at a uranyl concentration of 400 ppm, the developed ligand extracted approximately 59% of the UO_2^{2+} into the organic phase [13].

While various detection methods for UO_2^{2+} have been developed based on fluorogenic and colorimetric methods, studies on UO_2^{2+} adsorbents have received much less attention. We aim to synthesize an adsorbent, or uranyl-capture agent based on an organic–inorganic hybrid material because such compounds tend to have higher stability and controllable homogenous pore sizes.

Therefore, we designed and synthesized compound **1** (Figure 1). Compound **1** possesses four acetic acid groups as ligands for UO_2^{2+}. The spectroscopic properties of compound **1** were observed upon adding UO_2^{2+} via fluorometry, IR spectroscopy, and ^{1}H NMR spectroscopy. Furthermore, compound **1** was immobilized to **MPS** (mesoporous silica nanoparticles) to create an adsorbent for UO_2^{2+}. Herein, we report the spectroscopic properties of the compound **1**–UO_2^{2+} complex and the adsorption capacity of mesoporous silica nanoparticles loaded with compound **1** for UO_2^{2+} capture.

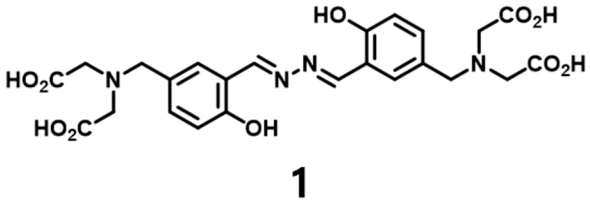

1

Figure 1. Chemical structure of compound **1**.

2. Materials and Methods

2.1. Reagents and Instruments

All reagents were purchased from Sigma-Aldrich (Buchs, Switzerland) and Tokyo chemical industry (Fukaya, Japan). The solvent was purchased from Samchun Pure Chemicals (Pyeongkaek, Korea) and used with further purification. ^{1}H and ^{13}C NMR spectra were obtained with a Bruker DRX 300 apparatus (Rheinstetten, Germany). The IR spectra were measured on a Shimadzu FT-IR 8400S instrument (Kyoto, Japan) by KBr pellet method in the range of 4000−1000 cm^{-1}. A JEOL JMS-700 mass spectrometer (Kyoto, Japan) was used to obtain the mass spectra. The UV−vis absorption and fluorescence spectra were obtained at 298 K with a Thermo Evolution 600 spectrophotometer (Waltham, MA, USA) and a RF-5301PC spectrophotometer (Kyoto, Japan), respectively. A PerkinElmer 2400 series (Waltham, MA, USA) was employed for the elemental analyses. The quantitative analysis was performed using ICP-DRC-MS (ELAN DRC II, PerkinElmer, Waltham, MA, USA). The morphological images were observed using a TEM (TECNAI G2 F30, FEI, Hillsboro, OR, USA).

2.2. Synthesis of Compound *1*

The compounds **1**–**4** were synthesized according to the reported method (Scheme S1) [14,15]. Compound **2** (2.56 mg, 0.4 mmol) was dissolved in THF (10 mL), followed by the addition of sodium hydroxide solution (10 mL, 0.8 M). The mixture was stirred at room temperature for 2 h. After completion of the reaction, the mixture was added to aq HCl solution (1 wt %) to give yellow precipitation, which was filtered off and dried under vacuum to yield compound **1** (121 mg, 57%). IR (KBr pellet) cm^{-1} 3424, 3014, 1728, 1495 1629, 1389, 1277, 1164; ^{1}H NMR (300 MHz, DMSO-d_6) δ 12.25 (s, 4H), 11.07 (s, 2H), 8.98 (s, 2H), 7.63 (d, J = 2.2 Hz, 2H), 7.40 (dd, J = 8.5, 2.2 Hz, 2H), 6.96 (d, J = 8.4 Hz, 2H), 3.78 (s, 4H), 3.42 (s, 8H); ^{13}C NMR (75 MHz, DMSO-d_6) δ 172.74, 162.82, 158.30, 134.37, 131.08, 130.12, 118.33, 116.99, 56.80, 53.96.; ESI-MS: calculated for $C_{24}H_{26}N_4O_{10}$, $[M - H]^-$ 529.16; found, 529.15; Anal. calcd for $C_{24}H_{26}N_4O_{10}$: C, 54.34; H, 4.94; N, 10.56; found: C 54.31, H 4.97, N 10.51.

2.3. Preparation of *MPS*

The **MPS** was synthesized according to the reported method [16]. 8.2 g of (1-Hexadecyl) trimethyl-ammonium bromide was dissolved in H_2O (600 mL). After stirring for 10 min, 1.6 mL of triethanolamine was added and the reaction mixture was heated. When the reaction temperature reached 80 °C, TEOS (tetra ethyl ortho silicate) (60 mL) was added and stirred for 1 h. The solvent of the reaction was removed by rotary evaporator and the resulting solid (including some water) was heated at 500 °C for 5 h by using a furnace.

2.4. Preparation of ***MPS-1***

0.1 g of compound **1** and 1 g of **MPS** in of acetonitrile (20 mL) were stirred for 10 min. The reaction mixture was refluxed at 80 °C for 24 h. After the reaction mixture was cooled to room temperature, the solid product was filtered and washed with 200 mL acetonitrile.

2.5. Photophysical Studies

The UV−vis absorption and fluorescence spectra were determined over the range 200−800 nm. The samples were prepared by dispersion in H_2O solution. The concentration of standard UO_2^{2+} solution was 100 ppb.

2.6. NMR Measurement

Compound **1** (2.65 mg, 0.005 mmol) and uranyl acetate (8.48 mg, 0.02 mmol) were dissolved in 0.5 mL and 0.1 mL of of DMSO-d_6 (0.5 mL) in DMSO-d_6 (0.1 mL), respectively. To NMR titration, the different amount of the uranyl acetate solution (12.5 μL, 25 μL, 37.5 μL, 50 μL) was added to compound **1** of DMSO-d_6 (0.5 mL).

2.7. ICP-MS

MPS-1 (1 mg, 3 mg, and 5 mg) were dispersed in aqueous solution containing UO_2^{2+}, Na^+, Mg^{2+}, Ca^{2+}, Cu^{2+}, Ag^+, Co^{2+}, Ni^{2+}, Mn^{2+} and Pb^{2+} (100 ppb) for 10 min. Mixture was added to H_2O (4 mL). The mixture solution was centrifuged and the supernatant solution was filtrated with syringe filter (PTFE, 0.45 μm). The collected solution was measured 3 times by ICP-MS.

3. Results and Discussion

3.1. Spectroscopic Properties of Complex ***1*** with UO_2^{2+}

Binding between UO_2^{2+} and specific ligands, such as cyclic peptides [17,18], porphyrins [19,20], and naphthobipyrrole [21,22], is well known. We prepared a salicyladazine derivative as a ligand for UO_2^{2+}. The salicyladazine derivative was synthesized starting from 2-hydroxybenzaldehyde. The diethyl 2,2′-azanediyldiacetate groups were designed on both sides of the compound to create a symmetric structure. As the final step, hydrochloric acid treatment of the precursor yielded the desired compound **1**. Compound **1** contains the acetic acid end group (–CH_2COOH) to form the binding site for UO_2^{2+} and was characterized via FT IR, ^{1}H and ^{13}C NMR, mass spectrometry, and elemental analysis (Figures S1, S2 and S3 in Supplementary Materials).

UV–vis spectroscopy was performed to confirm that a coordination bond between compound **1** and UO_2^{2+} resulted in a colorimetric change. Compound **1** was dissolved in an aqueous solution containing 1% of DMSO, and the UV–vis absorption spectrum was measured (Figure 2A). Before adding UO_2^{2+}, the π–π * absorption band of compound **1** appeared at around 300–350 nm. When UO_2^{2+} (from 0.5 to 3 equivalents in 0.5 equivalent steps) was added to compound **1**, the absorption peak intensities at 300 and 350 nm decreased until up to 2 equivalents of UO_2^{2+} were added. At 2.5 or more equivalents of UO_2^{2+}, the ligand-to-metal charge transfer absorption wavelength between compound **1** and UO_2^{2+} was observed at around 365–380 nm [23].

Figure 2B shows the photographs of the cuvettes used when UO_2^{2+} was added to compound **1** and irradiated under UV light. The change in fluorescence after more than 2 equivalents of UO_2^{2+} were added was visible to the naked eye. Compound **1** yielded an emission wavelength around 560 nm (excitation = 365 nm). When 0.5 equivalents of UO_2^{2+} were added to compound **1**, the fluorescence intensity decreased. The decrease in fluorescence was noticeable from 0.5 to 2 equivalents of UO_2^{2+}; however, the fluorescence intensity remained constant thereafter (Figure 2C). Figure 2D presents a plot of the fluorescence intensity vs. amount of UO_2^{2+} added. To determine the stoichiometric ratio

between compound **1** and UO_2^{2+}, we constructed a Job's plot using the fluorescence data and found a 1:2 binding ratio for compound **1**:UO_2^{2+} (Figure S4).

To investigate the chemical interactions between compound **1** and UO_2^{2+}, we used nuclear magnetic resonance (NMR) spectroscopy. We measured the ^{1}H NMR signal of compound **1** in DMSO-d_6 while increasing the UO_2^{2+} content (Figure 3). When 0.5 equivalent of UO_2^{2+} was added to compound **1** in DMSO-d_6, the proton peak (aromatic OH: 11.08 ppm) of compound **1** decreased and multiple new peaks were observed. When we added 1 equivalent of UO_2^{2+}, the ratio of the proton peaks of compound **1** and the resulting complex was 1:1. Because compound **1** has C2 symmetry, coordination of UO_2^{2+} occurs on one side of compound **1** (bound to two acetic acid ligands) and no coordination occurs on the other side of compound **1**. Upon additional UO_2^{2+} input (over 2 equivalents), all the peaks representing free compound **1** disappeared entirely. Therefore, compound **1** has a binding capacity of two UO_2^{2+} molecules in DMSO-d_6 (forms a 1:2 complex). This result is consistent with the Job's plot.

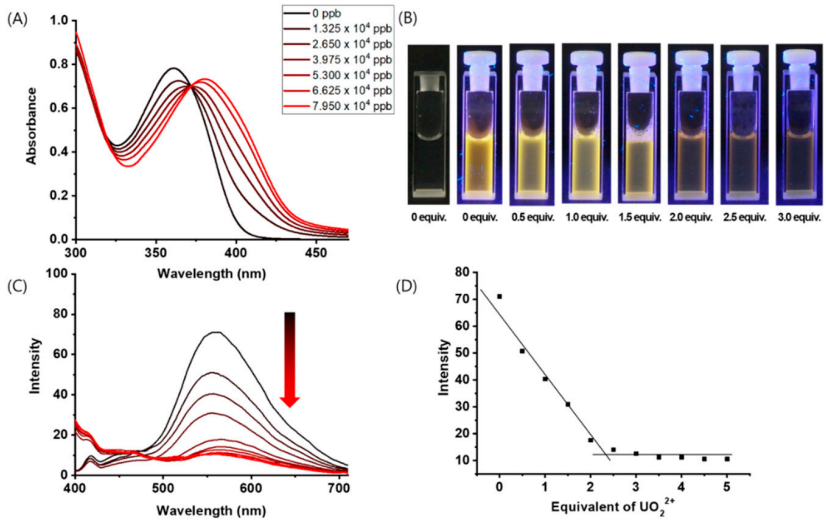

Figure 2. (**A**) UV–vis spectra of compound **1** (2.65×10^4 ppb) in DMSO/H_2O (1:99 *v*/*v*) containing various amounts of UO_2^{2+}. (**B**) Photographed cuvettes from (**A**) under UV light irradiation. (**C**) Fluorescence spectra of compound **1** (2.65×10^4 ppb) in DMSO/H_2O (1:99 *v*/*v*) containing various amounts of UO_2^{2+} (0–5 equivalents). (**D**) Plot of fluorescence intensity of (**C**) vs. amount of UO_2^{2+}.

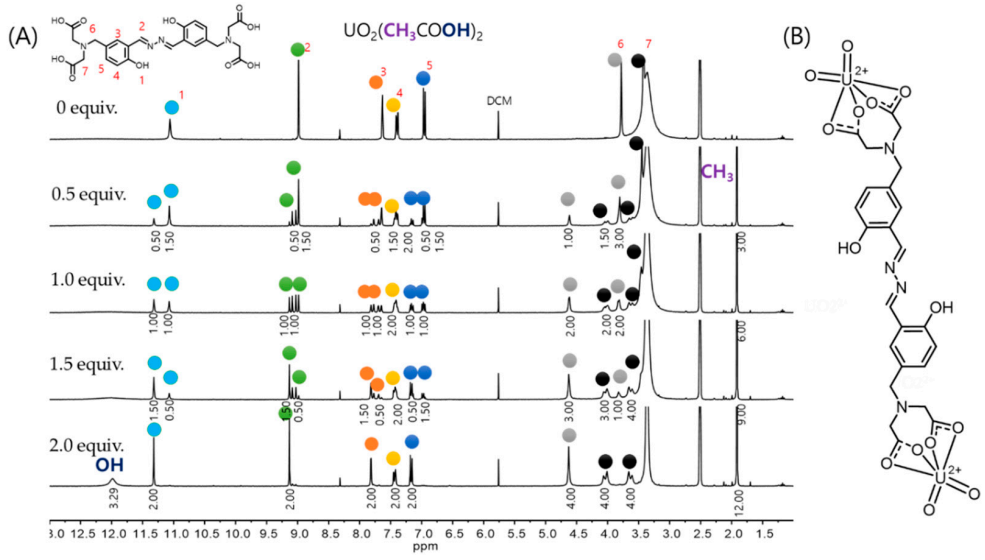

Figure 3. (**A**) ^{1}H nuclear magnetic resonance (NMR) spectra of compound **1** (10 mM) in DMSO-d_6 containing various equivalents of uranyl acetate. (**B**) Proposed structure of complex **1** with UO_2^{2+}.

The carbonyl oxygen (C=O) of the end group of acetic acids (–CH_2COOH) in compound **1** is well known to bind strongly to a radionuclide ion such as UO_2^{2+} by supplying electrons [23,24]. IR spectroscopy was used to classify the complex formation of compound **1** with UO_2^{2+}. As shown in Figure S5, the oxygen of the carboxylic acid carbonyl (C=O) in compound **1** before the addition of UO_2^{2+} produced a peak at 1728 cm^{-1}, whereas the C=O peak after the addition of UO_2^{2+} was shifted to 1557 cm^{-1}. This shift to a lower wavenumber is indicative of the C=O in compound **1** providing electrons in a dative bond to UO_2^{2+} and confirms that the carboxylic acid groups are employed in complex formation with UO_2^{2+}.

3.2. Immobilization of Compound *1* to Mesoporous Silica Nanoparticles

The morphology of mesoporous silica nanoparticle immobilized with **1** (**MPS-1**) was observed via transmission electron microscopy (TEM). The TEM image of **MPS-1** revealed a spherical structure with a narrow size distribution (circa 40 nm) (Figure 4A). Thermogravimetry analysis (TGA) was performed to determine the amount of compound **1** immobilized onto **MPS-1** (Figure 4B). At approximately 150 °C, the weight of **MPS-1** decreased by 4.2%. This mass reduction was attributed to moisture. At ~500 °C, compound **1** was pyrolyzed and the weight of **MPS-1** decreased to 86.8% (Figure S6). Thus, the amount of compound **1** introduced into **MPS-1** was 9% by weight (Figure 4B). Figure S7 presents the IR spectra of **MPS** and **MPS-1**; a C-H vibration peak of 2940 cm^{-1} was confirmed. This further supported the presence of compound **1** on the surface of the mesoporous silica nanoparticles. Under UV light irradiation, the filtered silica nanoparticles fluoresced blue, indicating that compound **1** was present on the mesoporous silica nanoparticle surface. Fluorescence spectra of **MPS-1** (2 mg) in water (2 mL) and **MPS-1** (2 mg) in 100 ppb UO_2^{2+} solution (2 mL) were also measured. (Figure 4C). In 3.5% NaCl aqueous solution of 2mL, we measured the fluorescence spectra of **MPS-1** (2 mg) and **MPS-1** (2 mg) in 100 ppb UO_2^{2+} solution, respectively (Figure S8). Fluorescence changes of **MPS-1** in the present of 100 ppb UO_2^{2+} in water or 3.5% NaCl aqueous solution were shown similar results. This means that **MPS-1** can bind UO_2^{2+} not only in water but also NaCl aqueous solution.

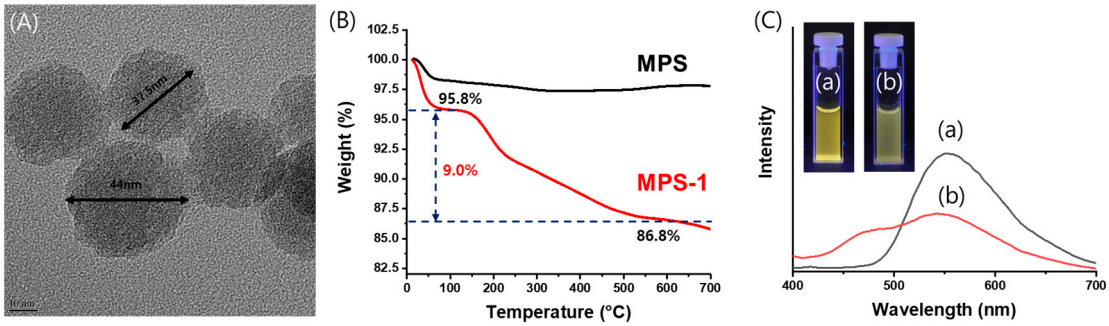

Figure 4. (**A**) Transmission electron microscopy (TEM) image of mesoporous silica (**MPS-1**) and (**B**) thermogravimetry analysis (TGA) thermogram of **MPS** (black) and **MPS-1** (red). (**C**) The photograph and the Fluorescence spectra of (**a**) **MPS-1** (2 mg) in water (2 mL) and (**b**) **MPS-1** (2 mg) in 100 ppb UO_2^{2+} solution (2 mL).

3.3. The Adsorption Capacity of *MPS-1* for UO_2^{2+}

The United States Environmental Protection Agency (US EPA) and the World Health Organization (WHO) have prescribed safe limits of UO_2^{2+} in drinking water at 30 ppb [25,26]. The adsorption capacity of **MPS-1** was tested by adding 1, 3, and 5 mg of **MPS-1** to 1 mL of 100 ppb UO_2^{2+} solution. After standing for 10 min, the solution was filtered through a 0.45-μm syringe filler and the UO_2^{2+} levels were determined by ICP-MS (experiment performed in triplicate). Calibration curves were obtained with dilute UO_2^{2+} solutions (0.1, 1, 10, 50, and 100 ng/L), and the linearity of the calibration curve was confirmed (correlation coefficient was 0.9974) (Figure S9). Figure 5 and Table S1 present the results of the UO_2^{2+} adsorption experiment using various amounts of **MPS-1**. The percentage of

UO_2^{2+} removed was 70%, 96%, and 95% for 1, 3, and 5 mg of **MPS-1**, respectively (RSD values all less than 15%). 1 mg of **MPS-1** was not sufficient for absorbing 100 ppb UO_2^{2+}. Using 3 or 5 mg of **MPS-1** removed 95% or more of the UO_2^{2+}; there was no statistically significant difference between the two absorbent dose amounts. In conclusion, **MPS-1** (even a small amount: 0.3 wt %) could reduce 100 ppb of UO_2^{2+} <5 ppb of UO_2^{2+}; this result would satisfy both EPA and WHO drinking water standards.

*3.4. Adsorption of UO_2^{2+} and Other Cations onto **MPS-1***

The elemental analysis of **MPS**, **MPS-1**, and UO_2^{2+}-adsorbed **MPS-1** was performed via TEM dispersive X-ray spectroscopy (EDX) (Figure S10). Nitrogen was observed in the EDX spectrum of **MPS-1**, thus providing evidence for the presence of compound **1** in **MPS-1**. In the EDX spectrum of UO_2^{2+}-adsorbed **MPS-1**, uranium was detected. This confirms our rationale in designing this adsorbent: UO_2^{2+} was bound to the compound **1** attached onto the surface of **MPS**.

We also confirmed the adsorption capacity of **MPS-1** (5 mg) for other metal ions, such as Na^+, Mg^{2+}, Ca^{2+}, Cu^{2+}, Ag^+, Co^{2+}, Ni^{2+}, Mn^{2+}, and Pb^{2+} (100 ppb) under the same conditions. Among the metal ions tested, 42.3% of Ca^{2+} was adsorbed onto the surface of **MPS-1**; for the remaining metal ions, <30% were adsorbed (Table S2). These findings suggest that **MPS-1** would be useful as an adsorbent for UO_2^{2+}.

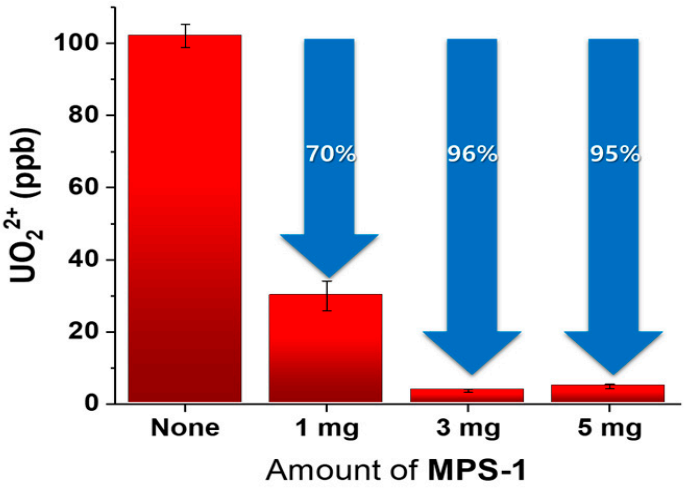

Figure 5. Result of UO_2^{2+} adsorption of **MPS-1** in 100 ppb UO_2^{2+} solution.

4. Conclusions

We synthesized the salicyladazine-based compound **1**, designed to be a uranyl ion capture ligand. Compound **1** formed a 1:2 complex with UO_2^{2+} as confirmed by the Job's plot. A fluorescence change was observed when UO_2^{2+} was bound to compound **1**. IR and NMR measurements were performed to identify compound **1** and the two UO_2^{2+} coordination sites. Compound **1** was immobilized into mesoporous silica (**MPS-1**); the resulting sorbent could remove 96% of the UO_2^{2+} from 1 mL of a 100-ppb UO_2^{2+} aqueous solution. A material was successfully developed that was capable of simultaneously absorbing uranyl ions and detecting their presence by fluorescence. We believe that this organic–inorganic hybrid material paradigm for detecting UO_2^{2+} will have a broad impact for the study on porous materials and their application.

Supplementary Materials: The following are available online at http://www.mdpi.com/2079-4991/9/5/688/s1. Scheme S1. Synthesis route of compound **1**; Figure S1. FT-IR spectrum of compound **1**; Figure S2. ^{1}H NMR spectrum of compound **1** in DMSO-d_6; Figure S3. ^{13}C NMR spectrum of compound **1** in DMSO-d_6; Figure S4. Job's plot for complex formed between compound **1** and UO_2^{2+}; Figure S5. FT-IR spectra of **1** and **1** with UO_2^{2+}; Figure S6. TGA thermogram of compound **1**; Figure S7. FT-IR spectra of (A) **MPS** and (B) **MPS-1**; Figure S8. Fluorescence spectra of (a) **MPS-1** (2 mg) in 3.5% NaCl solution (2mL) and (b) **MPS-1** (2 mg) with UO_2^{2+} solution (100 ppb) in 3.5% NaCl (2 mL); Figure S9. Linear equation of various concentrations of UO_2^{2+}; Figure S10. TEM EDX mapping

of (A) **MPS** (B) **MPS-1** and (C) **MPS-1** with UO_2^{2+}; Table S1. Adsorption Capacities of **MPS-1** for UO_2^{2+} (100 ppb) solution; Table S2. Adsorption Capacities of **MPS-1** (5 mg) with various metal ions (100 ppb) solution.

Author Contributions: Conceptualization, S.P. and J.P.; Data curation, S.P.; Formal analysis, S.P. and J.P.; Investigation, S.P. and J.P.; Methodology, J.P.; Project administration, J.H.L. and J.H.J.; Supervision, J.H.L., M.Y.C. and J.H.J.; Writing—Original draft, J.H.L.; Writing—Review & editing, J.H.L., M.Y.C. and J.H.J.

Funding: This research was supported by the NRF (2018R1A2B2003637, 2017M2B2A9A02049940 and 2017R1A4A1014595) supported by the Ministry of Education, Science and Technology, Korea. In addition, this work was partially supported by a grant from the Next-Generation BioGreen 21 Program (SSAC, Grant no. PJ013186052019), Rural Development Administration, Korea.

Conflicts of Interest: The authors declare no conflict of interest.

References

1. O'Loughlin, E.J.; Kelly, S.D.; Cook, R.E.; Csencsits, R.; Kemner, K.M. Reduction of Uranium(VI) by Mixed Iron(II)/Iron(III) Hydroxide (Green Rust): Formation of UO_2 Nanoparticles. *Environ. Sci. Technol.* **2003**, *37*, 721–727. [CrossRef] [PubMed]
2. Feng, M.-L.; Sarma, D.; Qi, X.-H.; Du, K.-Z.; Huang, X.-Y.; Kanatzidis, M.G. Efficient Removal and Recovery of Uranium by a Layered Organic–Inorganic Hybrid Thiostannate. *J. Am. Chem. Soc.* **2016**, *138*, 12578–12585. [CrossRef] [PubMed]
3. Asiabi, H.; Yamini, Y.; Shamsayei, M. Highly efficient capture and recovery of uranium by reusable layered double hydroxide intercalated with 2-mercaptoethanesulfonate. *Chem. Eng. J.* **2018**, *337*, 609–615. [CrossRef]
4. Wu, P.; Hwang, K.; Lan, T.; Lu, Y. A DNAzyme-Gold Nanoparticle Probe for Uranyl Ion in Living Cells. *J. Am. Chem. Soc.* **2013**, *135*, 5254–5257. [CrossRef]
5. Cao, X.-H.; Zhang, H.-Y.; Ma, R.-C.; Yang, Q.; Zhang, Z.-B.; Liu, Y.-H. Visual colorimetric detection of UO_2^{2+} using o-phosphorylethanolamine-functionalized gold nanoparticles. *Sens. Actuators B* **2015**, *218*, 67–72. [CrossRef]
6. Elabd, A.A.; Attia, M.S. A new thin film optical sensor for assessment of UO_2^{2+} based on the fluorescence quenching of Trimetazidine doped in sol gel matrix. *J. Lumin.* **2015**, *165*, 179–184. [CrossRef]
7. Xiao, S.J.; Zuo, J.; Zhu, Z.Q.; Ouyang, Y.Z.; Zhang, X.L.; Chen, H.W.; Zhang, L. Highly sensitive DNAzyme sensor for selective detection of trace uranium in ore and natural water samples. *Sens. Actuators B* **2015**, *210*, 656–660. [CrossRef]
8. Elabd, A.A.; Attia, M.S. Spectrofluorimetric assessment of UO_2^{2+} by the quenching of the fluorescence intensity of Clopidogrel embedded in PMMA matrix. *J. Lumin.* **2016**, *169*, 313–318. [CrossRef]
9. Zheng, S.; Wang, H.; Hu, Q.; Wang, Y.; Hu, J.; Zhou, F.; Liu, P. "Turn-On" fluorescent chemosensor based on β-diketone for detecting Th^{4+} ions in Aqueous Solution and application in living cell imaging. *Sens. Actuators B* **2017**, *253*, 766–772. [CrossRef]
10. Wen, J.; Huang, Z.; Hu, S.; Li, S.; Li, W.; Wang, X. Aggregation-induced emission active tetraphenylethene-based sensor for uranyl ion detection. *J. Hazard. Mater.* **2016**, *318*, 363–370. [CrossRef]
11. Harvey, P.; Nonat, A.; Platas-Iglesias, C.; Natrajan, L.S.; Charbonniere, L.J. Sensing Uranyl(VI) Ions by Coordination and Energy Transfer to a Luminescent Europium(III) Complex. *Angew. Chem. Int. Ed.* **2018**, *57*, 9921–9924. [CrossRef]
12. Lee, J.H.; Wang, Z.; Liu, J.; Lu, Y. Highly sensitive and selective colorimetric sensors for uranyl (UO_2^{2+}): Development and comparison of labeled and label-free DNAzyme-gold nanoparticle systems. *J. Am. Chem. Soc.* **2008**, *130*, 14217–14226. [CrossRef]
13. Sather, A.C.; Berryman, O.B.; Rebek, J. Selective recognition and extraction of the uranyl ion from aqueous solutions with a recyclable chelating resin. *Chem. Sci.* **2013**, *4*, 3601–3605. [CrossRef]
14. Zhang, S.; Sun, M.; Yan, Y.; Yu, H.; Yu, T.; Jiang, H.; Zhang, K.; Wang, S. A turn-on fluorescence probe for the selective and sensitive detection of fluoride ions. *Anal. Bioanal. Chem.* **2017**, *409*, 2075–2081. [CrossRef] [PubMed]
15. Gao, M.; Li, Y.; Chen, X.; Li, S.; Ren, L.; Tang, B.Z. Aggregation-Induced Emission Probe for Light-Up and in Situ Detection of Calcium Ions at High Concentration. *ACS Appl. Mater. Interfaces* **2018**, *10*, 14410–14417. [CrossRef]

16. Zhang, K.; Xu, L.L.; Jiang, J.G.; Calin, N.; Lam, K.F.; Zhang, S.J.; Wu, H.H.; Wu, G.D.; Albela, B.; Bonneviot, L.; et al. Facile large-scale synthesis of monodisperse mesoporous silica nanospheres with tunable pore structure. *J. Am. Chem. Soc.* **2013**, *135*, 2427–2430. [CrossRef] [PubMed]
17. Yang, C.-T.; Han, J.; Gu, M.; Liu, J.; Li, Y.; Huang, Z.; Yu, H.-Z.; Hu, S.; Wang, X. Fluorescent recognition of uranyl ions by a phosphorylated cyclic peptide. *Chem. Commun.* **2015**, *51*, 11769–11772. [CrossRef] [PubMed]
18. Starck, M.; Sisommay, N.; Laporte, F.A.; Oros, S.; Lebrun, C.; Delangle, P. Preorganized Peptide Scaffolds as Mimics of Phosphorylated Proteins Binding Sites with a High Affinity for Uranyl. *Inorg. Chem.* **2015**, *54*, 11557–11562. [CrossRef] [PubMed]
19. Sessler, J.L.; Seidel, D.; Vivian, A.E.; Lynch, V.; Scott, B.L.; Keogh, D.W. Hexaphyrin(1.0.1.0.0.0): An Expanded Porphyrin Ligand for the Actinide Cations Uranyl (UO_2^{2+}) and Neptunyl (NpO^{2+}). *Angew. Chem. Int. Ed.* **2001**, *40*, 591–594. [CrossRef]
20. Sessler, J.L.; Gorden, A.E.V.; Seidel, D.; Hannah, S.; Lynch, V.; Gordon, P.L.; Donohoe, R.J.; Drew Tait, C.; Webster Keogh, D. Characterization of the interactions between neptunyl and plutonyl cations and expanded porphyrins. *Inorg. Chim. Acta* **2002**, *341*, 54–70. [CrossRef]
21. Anguera, G.; Brewster, J.T.; Moore, M.D.; Lee, J.; Vargas-Zúñiga, G.I.; Zafar, H.; Lynch, V.M.; Sessler, J.L. Naphthylbipyrrole-Containing Amethyrin Analogue: A New Ligand for the Uranyl (UO_2^{2+}) Cation. *Inorg. Chem.* **2017**, *56*, 9409–9412. [CrossRef]
22. Brewster, J.T.; He, Q.; Anguera, G.; Moore, M.D.; Ke, X.-S.; Lynch, V.M.; Sessler, J.L. Synthesis and characterization of a dipyriamethyrin–uranyl complex. *Chem. Commun.* **2017**, *53*, 4981–4984. [CrossRef] [PubMed]
23. Marten-Ramos, P.; Costa, A.L.; Silva, M.R.; Pereira, L.C.J.; Pereira da Silva, P.S.; Seixas de Melo, J.S.; Martin-Gil, J. Luminescent properties of $[UO_2(TFA)_2(DMSO)_3]$, a promising material for sensing and monitoring the uranyl ion. *Mater. Res.* **2016**, *19*, 328–332. [CrossRef]
24. Du, N.; Song, J.; Li, S.; Chi, Y.-X.; Bai, F.-Y.; Xing, Y.-H. A Highly Stable 3D Luminescent Indium-Polycarboxylic Framework for the Turn-off Detection of $UO_2(^{2+})$, $Ru(^{3+})$, and Biomolecule Thiamines. *ACS Appl. Mater. Interfaces* **2016**, *8*, 28718–28726. [CrossRef] [PubMed]
25. 2018 Drinking Water Standards and Advisory Tables. Available online: https://www.epa.gov/dwstandardsregulations/2018-drinking-water-standards-and-advisory-tables (accessed on 29 April 2019).
26. Guidelines for Drinking-Water Quality, 4th ed. Available online: https://www.who.int/water_sanitation_health/publications/2011/dwq_guidelines/en/ (accessed on 29 April 2019).